

Pressure-induced changes in the optical properties of quasi-one-dimensional $\beta\text{-Na}_{0.33}\text{V}_2\text{O}_5$

Simone Frank and Christine A. Kuntscher*

Lehrstuhl für Experimentalphysik II, Universität Augsburg, D-86135 Augsburg, Germany

Ivan Gregora

*Institute of Physics, Academy of Sciences of the Czech Republic,
Na Slovance 2, 182 21 Prague 8, Czech Republic*

Touru Yamauchi and Yutaka Ueda

*Institute for Solid State Physics, University of Tokyo,
5-1-5 Kashiwanoha, Kashiwa, Chiba 277-8581, Japan*

(Dated: February 1, 2008)

The pressure-induced changes in the optical properties of $\beta\text{-Na}_{0.33}\text{V}_2\text{O}_5$ single crystals at room temperature were studied by polarization-dependent Raman and far-infrared reflectivity measurements under high pressure. From the changes in the Raman- and infrared-active phonon modes in the pressure range 9 - 12 GPa a transfer of charge between the different V sites can be inferred. The importance of electron-phonon coupling in the low-pressure regime is discussed.

I. INTRODUCTION

In solid state matter with complex crystal structure the distribution of charge on the various structural entities, like chains or ladders of polyhedra, generally is one key for understanding the observed electronic and magnetic properties. In the presence of strong electronic correlations, especially in systems with reduced dimensions, these systems often exhibit an ordering of the charge carriers or a charge disproportionation. In some rare cases superconductivity occurs in direct vicinity to the charge-ordered phase. The low-dimensional vanadate $\beta\text{-Na}_{0.33}\text{V}_2\text{O}_5$ is such an example: It shows a superconducting phase in the pressure range between 7 GPa to 9 GPa below ≈ 9 K.¹ For lower pressures a phase of charge ordering/charge disproportionation is found.^{1,2}

$\beta\text{-Na}_{0.33}\text{V}_2\text{O}_5$ crystallizes in a monoclinic tunnel-like structure built by three kinds of chains along the b axis which consist of three inequivalent vanadium sites. Along the b axis the edge-shared (V1) O_6 octahedra form a zigzag double chain. The (V2) O_6 octahedra form a two-leg ladder by corner sharing and the (V3) O_5 polyhedra form zigzag double chains. There are two possible sodium sites located in the tunnels along the b axis. They can be represented as a two-leg ladder along the b axis. For a sodium stoichiometry of 0.33 half of the sites is occupied. At room temperature the sodium atoms are statistically distributed over these sites.³ In Fig. 1 a projection of the crystal structure, the two types of chains, and the two-leg ladder formed by vanadium oxide polyhedra and octahedra are shown. Recent NMR studies in combination with theoretical investigations suggest that regarding the dominant electronic interactions the system is rather to be described as consisting of weakly coupled V2-V2 and V1-V3 ladders.^{2,4}

Dc resistivity measurements on $\beta\text{-Na}_{0.33}\text{V}_2\text{O}_5$ reveal a one-dimensional metallic character, with the lowest resis-

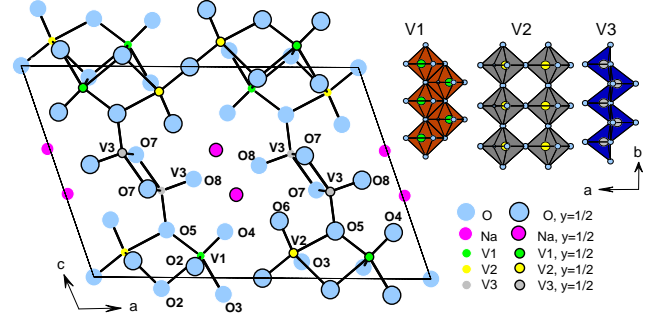


FIG. 1: (Color online) Crystal structure of $\beta\text{-Na}_{0.33}\text{V}_2\text{O}_5$ projected in the (010) plane.³ The vanadium oxide two-leg ladder as well as the two kinds of vanadium oxide chains are also shown.

tivity along the b axis, i.e., along the chain direction.^{5,6,7} This is in agreement with the optical properties of the material.⁸ For the polarization of the incident radiation along the chain direction, $\mathbf{E} \parallel b$, the reflectivity is high and a Drude contribution is found at room temperature, whereas in the perpendicular direction an insulating behavior is observed.

Up to now the nature of the pressure-induced superconductivity and the role of the distribution of charge for the superconducting phase are not clear. A first pressure-dependent study of the infrared reflectivity at room temperature revealed the electronic and lattice dynamical properties of $\beta\text{-Na}_{0.33}\text{V}_2\text{O}_5$ single crystals along different directions.^{9,10,11} The results of this study suggest the possible role of polaronic quasiparticles for the superconductivity: For $\mathbf{E} \parallel b$ a pronounced mid-infrared is observed, which was claimed⁸ to be of small-polaron origin. For pressures up to 12 GPa, this mid-infrared band shifts to smaller frequencies with increasing pressure, in agreement with small-polaron theory.^{9,10,11} Above 12 GPa this

trend is reversed. Further significant spectral changes are induced at around 12 GPa, like the development of additional excitations. It was suggested that the additional excitations are related to a redistribution of charge among the different V sites. Based on the infrared data a pressure-induced structural phase transition as an explanation for the additional excitations appeared unlikely but could not be ruled out.⁹

Raman spectroscopy, as a complementary tool to infrared spectroscopy, can give additional important information on the lattice dynamical properties. We therefore carried out a polarization-dependent Raman study on $\beta\text{-Na}_{0.33}\text{V}_2\text{O}_5$ single crystals under high pressure. We find significant changes in the Raman modes induced for pressures 9 - 12 GPa, in agreement with the pressure-dependent frequency positions of the far-infrared phonon modes. Several scenarios are considered as possible explanations for these findings, like structural phase transition, amorphization or charge redistribution. Furthermore, the possible relevance of electron-phonon coupling in $\beta\text{-Na}_{0.33}\text{V}_2\text{O}_5$ is discussed.

II. EXPERIMENT

The investigated $\beta\text{-Na}_{0.33}\text{V}_2\text{O}_5$ single crystals were grown according to Ref. 5. The sample quality was checked by infrared and dc resistivity measurements. Polarization-dependent Raman measurements at room temperature were carried out in backscattering geometry with a Renishaw System 1000 Micro-Raman Spectrometer equipped with a notch filter (130 cm^{-1} cut-off frequency) and a CCD multichannel detector. The 632.8 nm He-Ne laser line was used for excitation. To focus the beam on the sample an Olympus objective with a 20x magnification and a 21 mm working distance was attached to the microscope. The spot size on the sample was 5 μm . The studied frequency range extends from 140 cm^{-1} to 1200 cm^{-1} . For the high pressure experiment a diamond anvil cell equipped with type IIA diamonds was used. A small sample of the size of 80x80 μm^2 was cut and placed in the hole (150 μm) of a steel gasket. Finely ground KCl powder served as quasi-hydrostatic pressure transmitting medium. A small ruby chip was added to determine the pressure with the ruby luminescence method.¹² The reproducibility of the results was checked by two experimental runs.

In addition, we carried out polarization-dependent reflectivity measurements in the far-infrared range (200 - 650 cm^{-1}) at the infrared beamline of the synchrotron radiation source ANKA. A Bruker IFS 66v/S FT-IR spectrometer in combination with an infrared microscope (Bruker IRscope II), equipped with a 15x magnification objective was employed. For pressure generation up to 14 GPa a diamond anvil cell with type IIA diamonds and KCl powder as pressure medium were used. Reflectivity spectra R_{s-d} were measured at the interface between the sample and diamond anvil. Spectra taken at

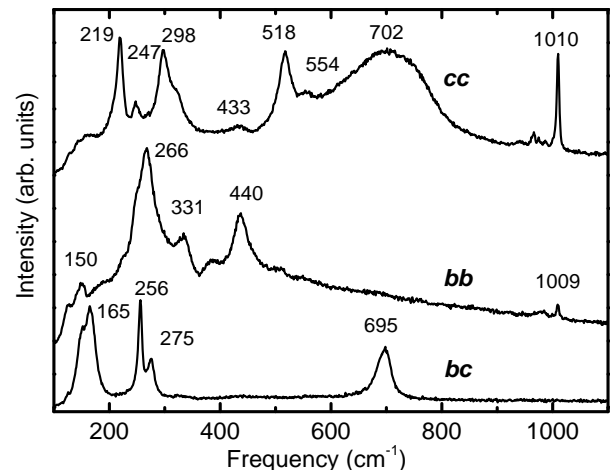


FIG. 2: Room-temperature Raman spectra of $\beta\text{-Na}_{0.33}\text{V}_2\text{O}_5$ at ambient pressure for the polarizations *cc*, *bb*, and *bc*. The spectra are shifted along the vertical axis for clarity.

the inner diamond-air interface of the empty cell served as the reference for normalization of the sample spectra. Schemes for the geometries of the sample and reference measurements are given in Ref. 9. Variations in source intensity were taken into account by applying additional normalization procedures. To obtain the frequency positions of the phonon modes, the reflectivity spectra were fitted with the Drude-Lorentz model combined with the normal-incidence Fresnel equation, taking into account the known refractive index of diamond.

III. RESULTS

A. Ambient-pressure Raman spectra

In Fig. 2 the room-temperature ambient-pressure Raman spectra of $\beta\text{-Na}_{0.33}\text{V}_2\text{O}_5$ are shown for parallel and crossed polarizations. The spectra are shifted along the vertical axis for clarity. For *cc* polarization seven modes (219, 247, 298, 433, 518, 554, 1010 cm^{-1}) and one broad peak-like structure at 702 cm^{-1} are observed. For *bb* polarization five strong modes (150, 266, 331, 390, 440, 1009 cm^{-1}) are found. The crossed *bc* polarization shows five modes (154, 165, 256, 275, 695 cm^{-1}) in the measured range. In Table I we list the different modes together with their assignments. The mode assignment is based on a comparison with Raman data of the closely related compound $\beta\text{-Ca}_{0.33}\text{V}_2\text{O}_5$.¹³ Both $\beta\text{-Ca}_{0.33}\text{V}_2\text{O}_5$ and $\beta\text{-Na}_{0.33}\text{V}_2\text{O}_5$ crystallize in the same monoclinic crystal structure, with a doubling of the unit cell in $\beta\text{-Ca}_{0.33}\text{V}_2\text{O}_5$ along the *b* direction due to an ordering of the Ca atoms (similar to the low-temperature phase of $\beta\text{-Na}_{0.33}\text{V}_2\text{O}_5$, see Refs. 14,15). Therefore, it is possible to compare the ambient-pressure Raman data of $\beta\text{-Na}_{0.33}\text{V}_2\text{O}_5$ with those of $\beta\text{-Ca}_{0.33}\text{V}_2\text{O}_5$.^{13,14,15} The phonon modes below 500 cm^{-1} originate from the bond

bending vibrations, while those at higher frequencies can be assigned to the stretching vibrations of the V-O polyhedra and octahedra. The highest-frequency modes at 1010 and 1009 cm^{-1} are attributed to the V3-O8 and V1-O4 bond stretching vibrations, respectively, since these are the shortest bonds.

The broad peak-like structure at 702 cm^{-1} for *cc* polarization is also observed in the Raman spectra of several closely related vanadate compounds, the most prominent one being the α' - NaV_2O_5 . α' - NaV_2O_5 was extensively studied because of its interesting low-temperature properties, namely a spin-Peierls-like phase transition at $T_c=35$ K with the simultaneous occurrence of charge disproportionation, lattice dimerization, and spin-gap formation.¹⁶ Despite the differences in the crystal structure of α' - NaV_2O_5 compared to that of β - $\text{Na}_{0.33}\text{V}_2\text{O}_5$ [and other members of the family β - $A_{0.33}\text{V}_2\text{O}_5$ ($A=\text{Sr}, \text{Ca}, \text{Na}, \dots$)]¹³ – the former being two-dimensional, the latter one-dimensional in nature – there are remarkable similarities in their Raman and optical conductivity spectra. These similarities are due to the fact that the electronic structures of the two compounds are based on similar structural units, as was shown by recent extended Hückel tight-binding calculations.⁴

In α' - NaV_2O_5 a similar broad Raman mode is found at around 650 cm^{-1} in *aa* polarization.^{17,18,19,20,21,22} Several scenarios have been proposed to explain this broad Gaussian-like band: (i) electric dipole transitions between the crystal field split V 3d levels, (ii) magnon scattering, and (iii) a mode due to strong electron-phonon coupling. Up to now, a consensus has not been reached on this issue. On the other hand, there are additional hints for the relevance of electron-phonon coupling in α' - NaV_2O_5 : the phonon modes close to the broad band are asymmetric and could be fitted with a Fano profile.^{17,20,23} Generally, such a mode asymmetry is assigned to the interaction between a discrete state (lattice vibration) and an electronic continuum. In comparison, in our ambient-pressure *cc* Raman spectrum of β - $\text{Na}_{0.33}\text{V}_2\text{O}_5$ an asymmetric profile of the mode located at 518 cm^{-1} , close to the broad band at around 702 cm^{-1} , is not obvious.

B. Pressure-dependent Raman and far-infrared reflectivity spectra

The results of the pressure-dependent Raman measurements are shown in Fig. 3. The spectra are shifted along the vertical axis for clarity. Due to the diamond absorption the intensity is reduced and therefore some of the ambient pressure modes are not detectable.

One important finding is that the Raman spectra do not change fundamentally in the whole studied pressure range. Most of the spectral features are present up to the highest applied pressure. The observed changes are continuous, and mainly consist of a weakening or broadening of the spectral features. Therefore, we can rule out an amorphization of the sample, in agreement with

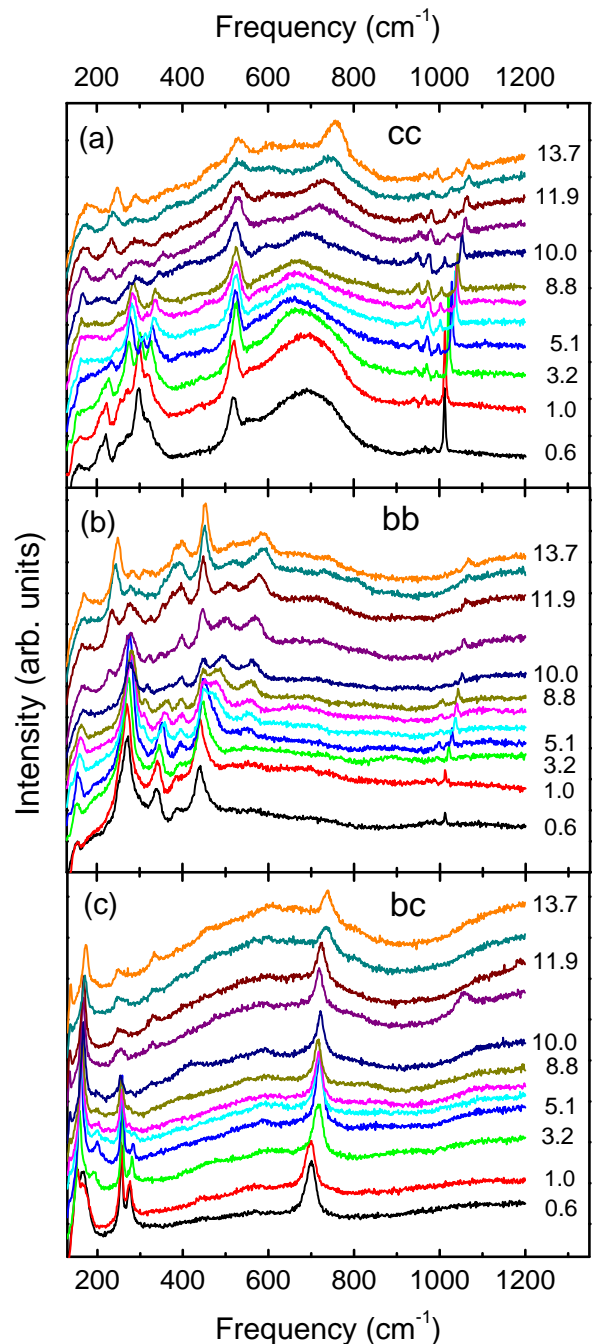


FIG. 3: (Color online) Pressure-dependent Raman spectra of β - $\text{Na}_{0.33}\text{V}_2\text{O}_5$ at room temperature for (a) *cc*, (b) *bb*, and (c) *bc* polarization. The spectra are plotted with an offset for clarity. The numbers give the applied pressures in GPa.

earlier conclusions based on our pressure-dependent mid-infrared data.⁹

A closer inspection of the spectra, however, reveals interesting pressure-induced changes: Almost all modes harden with increasing pressure, and the pressure-induced shift depends on the pressure range. In Fig. 4 the frequency shifts of the Raman modes with the most

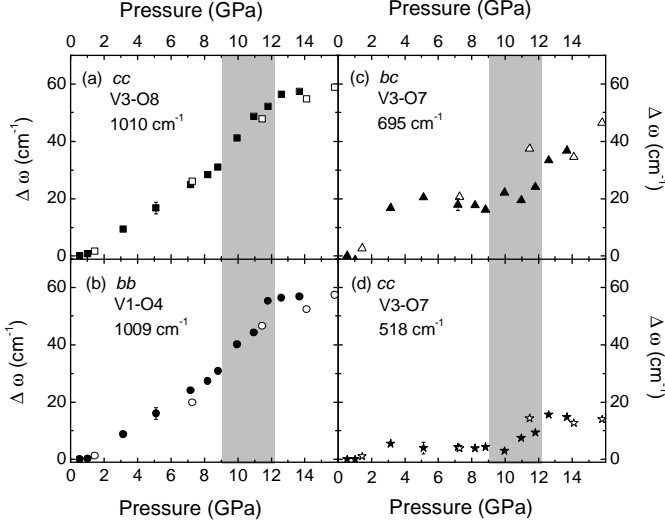


FIG. 4: Pressure dependence of the frequencies of several Raman modes of β - $\text{Na}_{0.33}\text{V}_2\text{O}_5$ at room temperature; full and open symbols denote results of two experimental runs. (a) V3-O8 bond stretching mode at 1010 cm^{-1} . (b) V1-O4 stretching mode at 1009 cm^{-1} . (c) V3-O7 stretching mode along the b axis at 695 cm^{-1} (d) V3-O7 stretching mode along the c axis at 518 cm^{-1} . The grey bars indicate the pressure range (9 - 12 GPa) with the most pronounced pressure-induced changes.

pronounced changes are shown. The frequency positions were obtained by fitting with Lorentzian functions. Below we describe the pressure-induced changes in more detail. All these changes are reversible upon pressure release.

For cc polarization [see Fig. 3(a)] the V3-O8 stretching mode located in the high-frequency range shifts linearly in the pressure range ≤ 9 GPa. The linear pressure coefficient was obtained by fitting the peak positions with the function $\omega(P) = A + B * P$, where P is the applied pressure. The so-obtained linear pressure coefficient B for this mode and the other modes is included in Table I. Above 9 GPa the V3-O8 stretching mode hardens strongly, and a saturation sets in above approximately 12 GPa [Fig. 4(a)]. In comparison, the V3-O7 stretching mode shows almost no pressure-induced frequency change up to approx. 10 GPa [Fig. 4(d)]. Between 10 and 12 GPa its frequency increases, and above 12 GPa the mode remains approximately constant. Furthermore, above 9 GPa a new Raman mode appears at a frequency of 230 cm^{-1} , which hardens with increasing pressure. The broad Raman peak at 702 cm^{-1} loses intensity with increasing pressure and evolves into a narrower peak, located at 758 cm^{-1} for the highest applied pressure.

For bb polarization [see Fig. 3(b)] the strongest modes at 266 and 440 cm^{-1} are not much affected by the pressure application regarding their frequency position: For the pressure range below 9 GPa they shift only by a few wavenumbers, and above 9 GPa their positions are

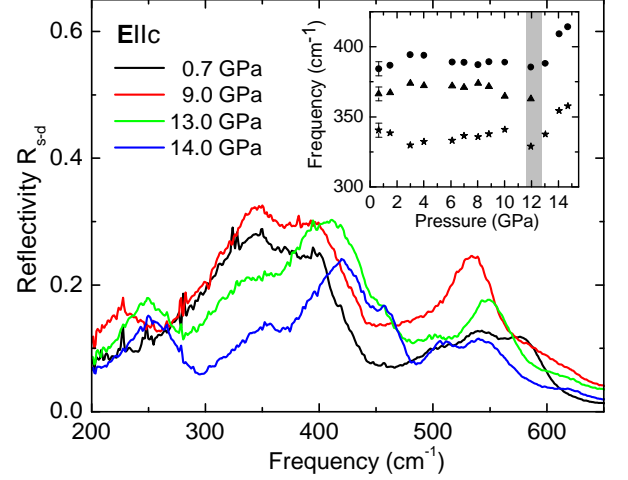


FIG. 5: (Color online) Far-infrared $\mathbf{E}||c$ reflectivity spectra R_{s-d} of β - $\text{Na}_{0.33}\text{V}_2\text{O}_5$ at room temperature for selected pressures. Inset: Frequency positions as a function of pressure for several phonon modes, obtained by fitting the reflectivity spectra with the Drude-Lorentz model; the grey bar indicates the pressure range with the most-pronounced pressure-induced changes.

approximately pressure-independent. The frequency of the V1-O4 stretching mode increases linearly with increasing pressure [see Fig. 4(b)] and remains constant above 12 GPa. It is interesting to note that the mode at 266 cm^{-1} appreciably loses intensity above 9 GPa. A further change induced at around 9 GPa is the appearance of a Raman mode at around 230 cm^{-1} , whose intensity increases with increasing pressure. In addition, two new modes (located at 500 and 550 cm^{-1}) appear above 5 GPa, shifting to higher frequencies with increasing pressure.

For bc polarization the V3-O7 stretching mode shows the strongest pressure dependence [see Figs. 3(c) and 4(c)]: After an initial shift, the mode is approximately pressure-independent up to 12 GPa, and above 12 GPa it hardens. Furthermore, above 9 GPa a weak, pressure-independent Raman mode appears at around 330 cm^{-1} .

In summary, for all the different studied polarizations the most pronounced changes in the Raman spectra are found in the pressure range between 9 and 12 GPa. This is in good agreement with our pressure-dependent far-infrared reflectivity measurements: In Fig. 5 the room-temperature reflectivity spectra R_{s-d} of β - $\text{Na}_{0.33}\text{V}_2\text{O}_5$ for the polarization $\mathbf{E}||c$ are shown for selected pressures. We obtained the frequency positions of the phonon modes by fitting the spectra with the Drude-Lorentz model combined with the normal-incidence Fresnel equation, taking into account the known refractive index of diamond. Several modes show marked changes at around 12 GPa, which is illustrated in the inset of Fig. 5: Here we show the pressure dependence of the frequency positions of the modes in the range $300 - 400\text{ cm}^{-1}$, which can be assigned to the polyhedral bending modes.²⁴ While the

frequency positions of these modes are almost pressure independent below 12 GPa, they significantly shift to higher energies above this pressure value. In addition, the oscillator strengths of the modes change at ≈ 12 GPa. At around the same pressure the changes in the Raman-active modes are observed, suggesting a conjoint interpretation of the effects.

IV. DISCUSSION

Earlier pressure-dependent mid-infrared data of β - $\text{Na}_{0.33}\text{V}_2\text{O}_5$ found new excitations induced at around 12 GPa, which were interpreted in terms of a redistribution of charge among the different V sites.⁹ Based on these data, a pressure-induced structural phase transition or amorphization of the sample appeared unlikely. The occurrence of a structural phase transition, however, could not be ruled out. According to our results, most of the Raman and far-infrared modes are present up to the highest applied pressure. Therefore, we can rule out an amorphization of the sample between 10 and 12 GPa. Furthermore, our results show that the structural units, i.e., the V-O polyhedra, remain intact up to the highest applied pressure.

In the pressure range 10 - 12 GPa several Raman-active modes show a significant change in their pressure-dependent frequency shifts. In general, the force constant and hence the frequency of a Raman mode are affected by the amount of charge on the ions involved in the vibrations.^{18,23} Accordingly, we interpret the changes observed in our Raman data in terms of a transfer of charge between the different V sites, setting in at 9 GPa and being completed at around 12 GPa. It is interesting to note, that the frequency of the V2-O1-V2 bending mode located at 440 cm^{-1} in *bb* polarization is hardly affected by the pressure application. Therefore, we speculate that the charge transfer occurs mainly among the V1 and V3 sites.

According to the above interpretation, the amount of charge located on the different structural entities [(V1) O_6 and (V2) O_6 octahedra, (V3) O_5 polyhedra] is changed between 9 and 12 GPa, which should influence the frequencies of the related infrared modes (like polyhedral bending and stretching modes). Indeed, this is demonstrated by the results of our far-infrared reflectivity data. Besides the frequency positions of the modes, their oscillator strengths are altered at around 12 GPa, which is also consistent with a pressure-induced rearrangement of the charges.

A further issue of interest concerns the relevance of electron-phonon coupling and possible formation of polaronic quasiparticles in β - $\text{Na}_{0.33}\text{V}_2\text{O}_5$. The pro-

nounced mid-infrared band observed by reflectivity measurements was attributed to polaronic excitations.⁸ Its pressure-induced redshift up to 12 GPa confirms this interpretation.^{9,10,11} Additional support of the importance of electron-phonon coupling can be inferred from the presence of the broad Raman mode in the *cc* Raman spectrum at around 700 cm^{-1} and its pressure dependence: Such a broad mode was also found in the Raman spectrum of the closely related α' - NaV_2O_5 . Here, its origin was related to the coupling of a phonon mode to an electronic state, among other possible scenarios.²² A similar mechanism based on electron-phonon coupling might also lead to the broad Raman mode in the present material. The mode is clearly visible in the Raman spectrum of β - $\text{Na}_{0.33}\text{V}_2\text{O}_5$ at ambient pressure, but weakens with increasing pressure and seems to have disappeared completely above ≈ 10 GPa. In the same pressure range (10 - 12 GPa) the presumable polaronic band in our mid-infrared reflectivity spectra^{9,10,11} changes its character. These findings suggest that electron-phonon coupling is indeed important in β - $\text{Na}_{0.33}\text{V}_2\text{O}_5$, at least up to ≈ 12 GPa.

V. SUMMARY

Our polarization-dependent Raman and far-infrared reflectivity spectra of β - $\text{Na}_{0.33}\text{V}_2\text{O}_5$ single crystals under pressure show significant changes in the phonon modes for pressures 9 - 12 GPa. Since most of the spectral features are present up to the highest applied pressure, a pressure-induced amorphization of the sample between 10 and 12 GPa can be ruled out. Furthermore, the structural units, i.e., the V-O polyhedra, remain intact up to the highest pressure. The observed pressure-induced changes in the optical properties can be related to a pressure-induced transfer of charge among the different V sites. The presence of the broad Raman mode in *cc* polarization below ≈ 12 GPa suggests the relevance of electron-phonon coupling in the low-pressure range.

Acknowledgments

We thank G. Untereiner for technical assistance. We acknowledge the ANKA Angströmquelle Karlsruhe for the provision of beamtime and we would like to thank D. Moss, Y.-L. Mathis, B. Gasharova, and M. Süpfle for assistance using beamline ANKA-IR. Financial support by the DAAD and the Deutsche Forschungsgemeinschaft through the Emmy Noether-program and SFB 484 is gratefully acknowledged.

* Email: christine.kuntscher@physik.uni-augsburg.de

¹ T. Yamauchi, Y. Ueda, and N. Môri, Phys. Rev. Lett. **89**,

- 057002 (2002).
- ² M. Itoh, I. Yamauchi, T. Kozuka, T. Suzuki, T. Yamauchi, J.-I. Yamaura, and Y. Ueda, *Phys. Rev. B* **74**, 054434 (2006).
 - ³ A.D. Wadsley *Acta Cryst.* **8**, 695 (1955)
 - ⁴ M.-L. Doublet, and M.-B. Lepetit, *Phys. Rev. B* **71**, 075119 (2005).
 - ⁵ H. Yamada and Y. Ueda, *J. Phys. Soc. Jpn.* **68**, 2735 (1999).
 - ⁶ M. Heinrich, H.-A. Krug von Nidda, R. M. Eremina, A. Loidl, Ch. Helbig, G. Obermeier and S. Horn, *Phys. Rev. Lett.* **93**, 116402 (2004).
 - ⁷ Y. Ueda, H. Yamada, M. Isobe, and T. Yamauchi, *J. Alloys Compd.* **317-318**, 109 (2001).
 - ⁸ C. Presura, M. Popinciuc, P. H. M. van Loosdrecht, D. van der Marel, M. Mostovoy, T. Yamauchi and Y. Ueda, *Phys. Rev. Lett.* **90**, 2, 026402 (2003).
 - ⁹ C. A. Kuntscher, S. Frank, I. Loa, K. Syassen, T. Yamauchi, and Y. Ueda, *Phys. Rev. B* **71**, 220502(R) (2005).
 - ¹⁰ C. A. Kuntscher, S. Frank, I. Loa, K. Syassen, T. Yamauchi, and Y. Ueda, *Physica B* **378-380**, 896-897 (2006).
 - ¹¹ C. A. Kuntscher, S. Frank, I. Loa, K. Syassen, F. Lichtenberg, T. Yamauchi, and Y. Ueda, *Infrared Physics & Technology* **49**, 88 (2006).
 - ¹² H. K. Mao, J. Xu, and P.M. Bell, *J. Geophys. Res. [Atmos.]* **91**, 4673 (1986).
 - ¹³ Z. V. Konstantinović, M. J. Popović, V. V. Moshchalkov, M. Isobe and Y. Ueda, *J. Phys. Cond. Matter* **15**, L139-L145 (2003).
 - ¹⁴ M. Isobe and Y. Ueda, *Mol. Cryst. Liq. Cryst.* **341**, 1075 (2000).
 - ¹⁵ J. I. Yamura, M. Isobe, H. Yamada, T. Yamauchi, and Y. Ueda, *J. Phys. Chem. Solids* **63**, 957 (2002).
 - ¹⁶ M. Isobe and Y. Ueda, *J. Phys. Soc. Jpn.* **65**, 1178 (1996); K. Ohwada, Y. Fujii, Y. Katsuki, J. Muraoka, H. Nakao, Y. Murakami, H. Sawa, E. Ninomiya, M. Isobe, and Y. Ueda, *Phys. Rev. Lett.* **94**, 106401 (2005) and references therein.
 - ¹⁷ M. J. Konstantinović, Z. V. Popović, V. V. Moshchalkov, C. Presura, R. Gajić, M. Isobe, and Y. Ueda, *Phys. Rev. B* **65**, 245103 (2002).
 - ¹⁸ W. S. Bacsa, R. Lewandowska, A. Zwick, and P. Millet, *J. Phys. Rev. B* **61**, R14885 (2000).
 - ¹⁹ S. A. Golubchik, M. Isobe, A. N. Ivlev, B. N. Mavrin, M. n. Popova, A. B. Sushkov, Y. Ueda, and A. N. Vesil'ev, *J. Phys. Soc. Jpn.* **66**, 4042 (1997).
 - ²⁰ I. Loa, U. Schwarz, M. Hanfland, R. K. Kremer, and K. Syassen, *phys. stat. sol. (b)* **215**, 709 (1999).
 - ²¹ M. J. Konstantinović, K. Ladavac, A. Belić, A. N. Vesil'ev, M. Isobe, and Y. Ueda, *J. Phys.: Condens. Matter* **11**, 2103 (1999).
 - ²² M. Fischer, P. Lemmens, G. Els, G. Güntherodt, E.Y. Sherman, E. Morré, C. Geibel, and F. Steglich *J. Phys. Rev. B* **60**, 7284 (1999).
 - ²³ Z. V. Popović, M. J. Konstantinović, R. Gajić, V. N. Popov, M. Isobe, Y. Ueda, and V. V. Moshchalkov, *Phys. Rev. B* **65**, 184303 (2002).
 - ²⁴ K. Thirunavukkuarasu, F. Lichtenberg, and C. A. Kuntscher, *J. Phys.: Condens. Matter* **18**, 9173 (2006).

TABLE I: Room-temperature Raman modes of β -Na_{0.33}V₂O₅ with their linear pressure coefficients, obtained by fitting their frequency position with the expression $\omega(P) = A + B * P$, and their assignment. Modes marked with an asterisk (dagger) appear (disappear) in the pressure range 9 - 12 GPa.

geometry	frequency ω (cm ⁻¹)	B for P \leq 9GPa (cm ⁻¹ /GPa)	B for 9GPa<P \leq 12GPa (cm ⁻¹ /GPa)	B for P>12GPa (cm ⁻¹ /GPa)	assignment
<i>cc</i>	230*		6.5	6.5	V3-O7 <i>c</i> axis stretching V3-O8 stretching
	298 [†]	2.5			
	518	0.3	4.5	-0.8	
	1010	3.8	6.0	0.6	
<i>bb</i>	230*				V2-O1-V2 bending
	266	1.4	0.2	0.2	
	331 [†]	2.8			
	390	0.1	0.1	0.1	
	440	1.7	-1.9	1.4	
	500*				V1-O4 stretching
	550*				
	1009	3.7	7.7	0.7	
<i>bc</i>	138*				V3-O7 <i>b</i> axis stretching
	154	1.2	1.2	1.2	
	165				
	256	0.1	0.1	0.1	
	275 [†]	1.8			
	330*				
	695	0.5	1.9	-0.6	